Anbar Journal of Engineering Science (AJES)
P-ISSN: 1997-9428; E-ISSN: 2706-7440

Vol. 12 , No. 2 (2021) , pp. 177 ~192
DOI: 10.37649/aengs.2021.171186

Anbar Journal Of Engineering Science©

journal homepage: http://www.uoanbar.edu.iq/Evaluate/

Unviersty of Anbar

Torsional Capacity of Composite Reinforced Concrete Beams with Stirrup Connectors

Dolfocar Ali Usamah Witwit, Prof. Dr. Nabeel Abdulrazzaq Jasim
Civil Engineering Department, College of Engineering, Basra University, Basra, Iraq

PAPER INFO

Paper history:

Received: 24/8/2021
Received in revised form: 25/9/2021
Accepted: 7/10/2021

Keywords:

CRC beam, Torsion,
Partial shear connector,
stirrup shear connector.

ABSTRACT

New composite reinforced concrete beams, in which reinforced concrete component is connected to steel T-section, are proposed. The shear connection between the two components, the reinforced concrete and the T-section, is provided by the stirrups that are required for the reinforced concrete component to resist the applied shear. Experimental tests in addition to numerical analysis were conducted to determine the behaviour and strength of such beams under pure torsion. Full scale one conventional reinforced concrete beam, T1, and two composite reinforced concrete ones, T2 and T3, were tested. The degree of shear connection between the two components of beams T2 and T3 was changed by varying the number of stirrups which are used as shear connectors. The experimental results revealed approximately same torsional stiffness for the three beams at the uncracked concrete stage. The torsional strength of the composite reinforced concrete beams was greater than that of ordinary reinforced concrete one by 11% and 27% for beams T2 and T3, respectively. Three-dimensional finite element analysis was conducted using program ABAQUS. To model the shear connection in composite reinforced concrete beam, the stirrups were connected to the web of the steel T-section by springs at the location of the stirrups. Good agreement is obtained between the results of the experimental tests and the finite element analysis. The ratios of experimental results to those of finite element analysis for torsional strength are approximately one. Under the pure torsion loading the degree of shear connection is found to have no effect on torsional capacity of beams.

1 Introduction

The method of combining steel and concrete, designated composite reinforced concrete CRC, was proposed in 1971[Taylor, 1979]. It was so called since it is a combination of composite construction and reinforced concrete.

In any comparison of different construction modes, the total cost, including the cost of the structural material and the cost of construction, is the governing matter. CRC combines the material advantages of reinforced concrete with the constructional advantages of normal composite construction [Taylor, 1977]. From material viewpoint the reinforced concrete is cheaper because the steel, the most expensive material, is used much more efficiently close to the soffit of beam. However, from the construction viewpoint, normal composite construction is the cheaper because the steel framework can be quickly built and used in

* Corresponding author. : Nabeel Abdulrazzaq Jasim ; : Nabeel.Jasim@gmail.com ; +9647724567882

constructing the concrete floor, especially when precast units or profiled steel sheets are used to spanning between the steel beams to act as formwork [Taylor, 1979].

The cross section of a CRC beam consists of a steel channel at the soffit of the beam connected to reinforced concrete by shear connectors, Figure (1-a). The shear connectors may be conventional studs welded to the web of channel section, transvers bolts [Taylor et al., 1974] passing through holes in the flanges of the channel or transvers bars [Taylor, 1977] placed through holes in the flanges of the channel.

Although the number of shear connectors was reduced in CRC, however, their cost is quite large. Recently, new form of CRC has been proposed [Dolfocar, 2021]. In the new structural material, the steel channel section was replaced by steel T-section and the shear stirrups of reinforced concrete were utilized to act as shear connectors. The steel T-section is better than the channel section in supporting the form for casting the concrete floor. Also, while in the new system no additional shear connectors are required, the preparation for connecting the steel T-section to the reinforced concrete needs only drilling holes in the web of the steel T-section through which the stirrups pass. To facilitate the construction, each stirrup was made from two C-shaped parts as shown in Figure (1-b).

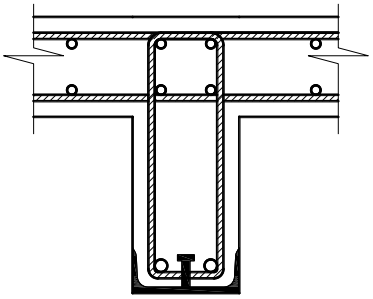

(a) Taylor's section

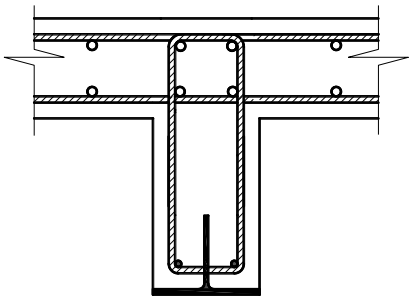

(b) Proposed section

Figure (1) CRC section

Witwit and Jasim [Dolfocar and Nabeel, 2021] investigated the behaviour under sagging and hogging bending moments of beams made of the proposed new CRC. The beams were tested under four-point loading. The effect on bending strength of beams of different degrees of shear connection was investigated.

There is no experimental research work on behaviour of CRC beams under torsion or combined flexure and torsion. However, experimental test on normal composite beams under torsion revealed that the contribution of the steel I-section towards the torsional strength of the composite beams is negligible. Hence, the torsional strength of such beams was determined as strength of the concrete slab only [Ghosh and Mallick, 1979].

This paper describes tests conducted on beams made of the new CRC under pure torsion. The behaviour and strength of such beams are attempted to be determined experimentally. Nonlinear finite element analysis is also conducted to study the behaviour of the beams up to failure. The results of the finite element analysis are compared with those obtained from the experimental tests.

2 Experimental work

2.1 Test beams

As a part of this study, experimental tests were conducted on two full scale CRC beams and one R.C beam to investigate the torsional behaviour of the beams. Each beam has a length of 3 m with effective torsional span of 2.6 m. The cross section of the beams was rectangular of

175 mm width and 350 mm depth. The beams were of Z-shape in plan, i.e. they were provided with end diaphragms to apply the load by which the torque is created. The cross section of CRC and RC beams was designed to be able to resist a positive (sagging) bending moment of 71.5 kN.m, a negative (hogging) bending moment of 95.8 kN.m, a shearing force of 125 kN. and twisting moment of 12 kN.m. These values of the applied moments and forces were chosen since the tested beams are a part of a complete research program on horizontally curved CRC beams [Dolfocar, 2021]. The beams section was designed as singly reinforced concrete according to the requirements of ACI318-14 code. The steel T-section was considered as a traditional reinforcement. The effective depth of the section for the positive bending moment was calculated to the centroid of the T-section. The details of tested beams are shown in Table (1) and Figure (2).

The stirrups were designed for combined shear and torsion. When all stirrups were used as shear connectors, as in beam T2, it was designated as beam with 100% degree of shear connection. The total number of stirrups was 43. To change the degree of shear connection, alternate stirrups were used as connectors in beam T3 resulting in a total of 21 stirrup connectors. This beam was designated as beam with 48.8% (=21/43×100) degree of shear connection.

Table 1 Description of the specimens

Specimen designation	Degree of interaction % (No. of stirrups)	Dimensions (mm)	
		Depth	Width
T1	R.C	350	175
T2	100 (43)	350	175
T3	48.8 (21)	350	175

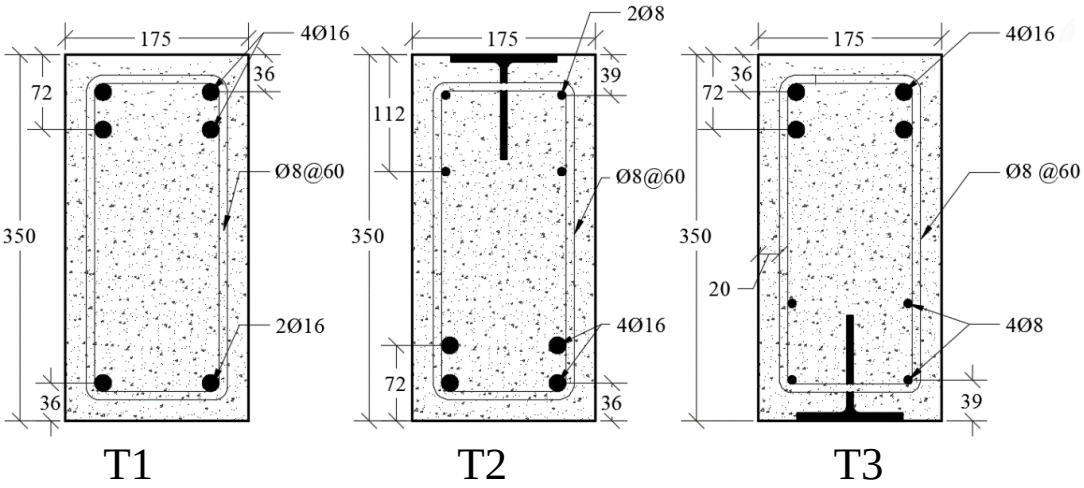

All dimensions are in millimetres
Figure (2) Cross-section details

2.2 Material

The concrete mix was made with Portland cement, natural sand and crushed gravel of 19 mm maximum size. Superplasticizer was made to obtain good workability of concrete for the required compressive strength. The properties of concrete are given in Table 2. The concrete control specimens were prepared and cured in the same manner as the test beams, and they were tested on the same day.

Steel T-section was used to fabricate the test beams. The section dimensions were 100 mm flange width with 7 mm thickness and 100 mm total depth with 5 mm web thickness.

Coupon tension tests were carried out on specimens cut from the flange and web of the section. The average properties of steel are shown in Table 2.

The longitudinal reinforcement and stirrups were of 16 mm and 8 mm deformed bars. Tension tests were carried out on specimens cut from the used quantity and the average properties obtained for the two dimeters are shown in Table 2.

Table 2 Details of material used in the CRC beams

Material	Property	Value
Concrete	Elastic modulus, MPa	25570
	Poisson's ratio	0.2
	Compression strength (cylinder), MPa	29.6
16 mm reinforcement bars	Elastic modulus, MPa	201282
	Poisson's ratio	0.3
	Ultimate tensile strength, MPa	636
	Yield strength, MPa	527
8 mm reinforcement bars	Elastic modulus, MPa	202150
	Poisson's ratio	0.3
	Ultimate tensile strength, MPa	490
	Yield strength, MPa	314
Steel T-section	Elastic modulus, MPa	204263
	Poisson's ratio	0.3
	Ultimate tensile strength, MPa	508
	Yield strength, MPa	376

2.3 Test setup, instrumentation and test procedure

The test setup is shown in Figures (3) to (6). A test rig was built with the aim to subject a pure torsion. The main portion of the beam specimen, between the two diaphragms, was supported on rollers parallel to the longitudinal axis of the beam to permit rotation of the diaphragm. The roller was placed between two steel plates of dimensions 175×175×20 mm as shown in Figure (3). Each diaphragm was equipped with 50-ton hydraulic cylinder connected to 35 MPa hand hydraulic pump, as shown in Figure (4-a). Flow control valve was used to avoid any displacement difference between the two diaphragms. The applied load was measured by a load cell. The applied torque was calculated by multiplying the load by the distance between the centre of loading plate and the roller support, which is set to 656 mm.

The angle of twist was measured by the use of dial gauges located on the diaphragms at a distance of 560 mm from the roller support. The angle of twist was calculated by dividing the recorded readings of the dial gauges (in mm) by the distance 560 mm. Two dial gauges were also installed on the side of the beam section distance 200 mm apart at the mid-length of the beam, as shown in Figures (3) and (5). These two dial gauges were used to ensure zero twist of this section.

Electrical resistance strain gauges were used to measure the strains in concrete and steel. Strain gauges with gauge length of 60 mm were used for concrete (as shown in Figure (4-c)) and gauge length of 5 mm for the steel T-section (as shown in Figure (4-d)). Two strain gauges were installed on concrete on the top face of the beams section to measure the longitudinal strains. Two strain gauge rosettes were also used (as shown in Figure (4-b)). One was attached to the concrete on the side of the beam section and the other was attached to the soffit of the flange of the steel T-section. The strain in reinforcement was assumed to be equal to the strain on the concrete surface at the location of reinforcement for both longitudinal bars and stirrups.

The beams were tested with the loads applied incrementally. After each increment all instrument readings were recorded and cracks were marked. Failure load was defined as the load at which a torsional rupture of concrete occurred and the twisting was increasing under

constant load. Figure (4-e) shows the strain gauge data logger and load cell data logger.

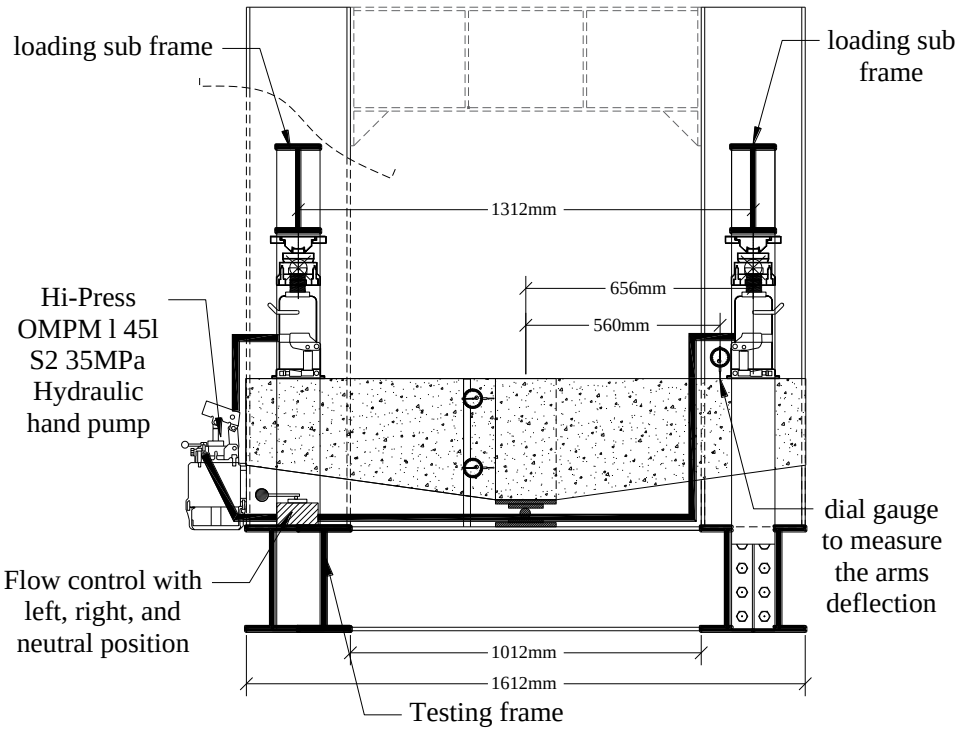

Figure (3) Setup for the torsion test (Side view)

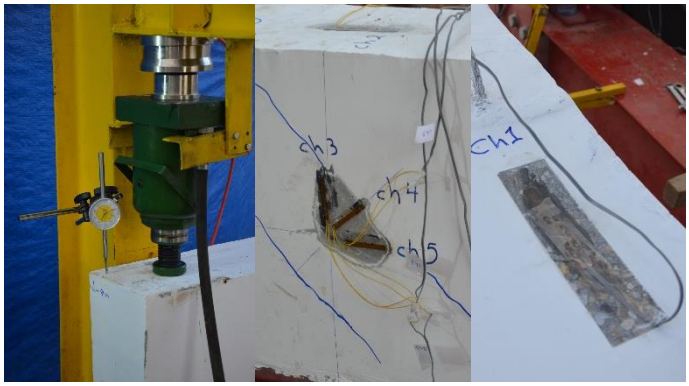

(a) (b) (c)

(d) (e)

Figure (4) Test equipment (a) loading piston load cell and dial gauge to measure the arm deflection, (b) strain gauge rosette, (c) Concrete TML Strain gauge model PL-60-11-3LIC, (d) Steel TML Strain gauge model FLA-5-11-3LJC, and (e) strain gauge data logger, and load cell data logger)

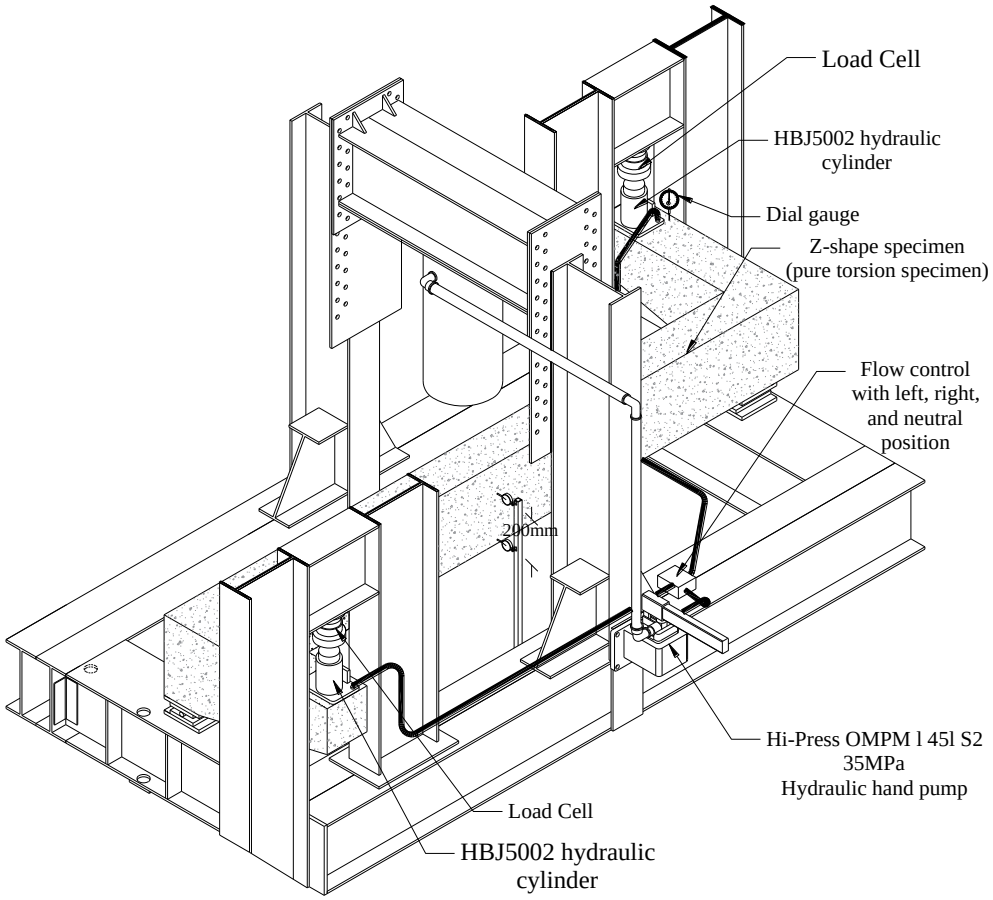

Figure (5) Setup for the torsion test (Three-dimensional view)

Figure (6) Setup for the torsion test (Testing rig, strain gauge data logger, and load cell data logger)

2.4 Failure modes

The reinforced concrete beam T1 suffered excessive spiral cracks that appeared at torque of 8.44 kN.m. No new cracks appeared after torque equal to 14.37 kN.m. The existing cracks

continued to widen and increase in length until the beam reaches its ultimate torsional strength of 19.11 kN.m at which the load starts decreasing due to the large twisting of the beam Figure (7) shows beam T1 after failure. The strain in the 8 mm stirrups reached its yield value at torque equal to 12.91 kN.m. The longitudinal 16 mm reinforcement started yielding at torque equal to 18.59 kN.m. Thus, the beam can be described as completely under-reinforced beam because the longitudinal and transverse reinforcement attained their yield strain.

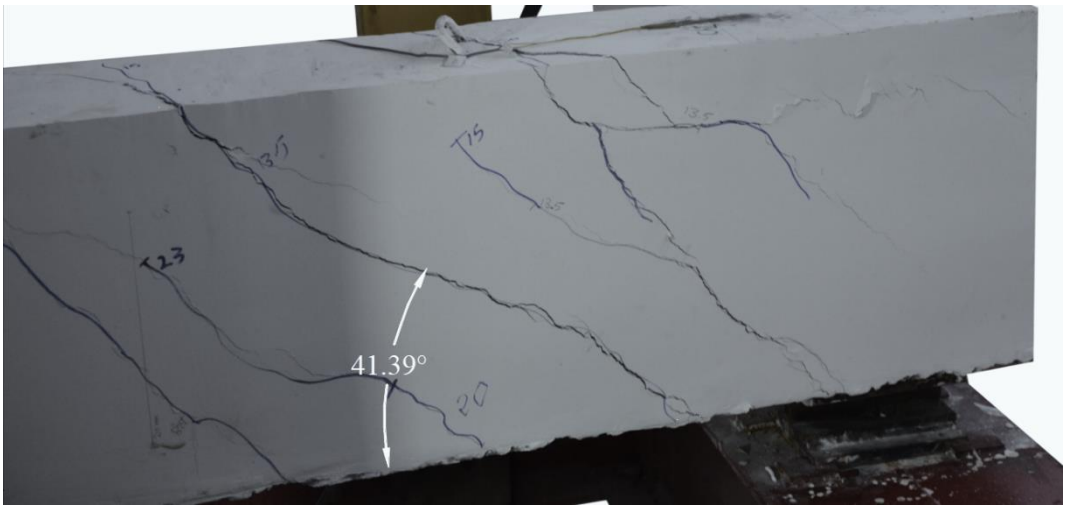

Figure (7) Specimen T1 after failure

In CRC beam T2, with 100% degree of shear connection between the steel T-section and concrete, cracking started at a torque equal to 7.9 kN.m. The cracks were spiral in shape along the length and no new cracks appeared after torque equal to 12.4 kN.m. The existing cracks continued to widen and increase in length until the beam reached its ultimate torsional strength of 21.25 kN.m. Figure (8) shows beam T2 after failure. The failure was due to the increase in spiral cracks width. When the torque reached its maximum value, the concrete cover was crushed as shown in Figure (8). Upon further inspection, it was found that the two parts of the stirrups were pulled apart from each other pushing the concrete cover outward. From the strain gauge rosette readings, it was found that the principal strain in the steel T-section has reached its yield value at torque equal to 16.92 kN.m. The strain in the 8 mm stirrups reached its yield value at torque equal to 17.64 kN.m. Thus, the beam is also completely under-reinforced.

Figure (8) Specimen T2 after failure

In CRC beam with 48.8% degree of shear connection the cracks started at torque equal to 9.38 kN.m and no new cracks appeared after torque equal to 23.75 kN.m. The beam maximum torque was 24.25 kN.m which is 1.14 times that of beam T2. The cracks were spiral and distributed along the beam more than that of T2, as shown in Figure (9). The strain in the 8 mm stirrups reached its yield value at torque equal to 20.5 kN.m. The steel T-section did not yield up to failure torque, so the beam can be described as partially over-reinforced. Table 3 summarizes the results for the group of specimens. It can be seen that the CRC beams have more torsional capacity than that of the RC beam T1. Also, the maximum torque for the CRC beam T3 with 48.8% degree of shear connection is 1.14 times that of beam T2 with 100% degree of shear connection. This may be due to the use of more closed continuous stirrups in specimen T3, whereas all stirrups consist two parts of c-shape.

Figure (9) Specimen T3 after failure

2.5 *Torsional moment-angle of twist behaviour*

Figures (9) to (11) depict the torsional moment-angle of twist relationships for the three beams tested in this study. The figures show that the linear behaviour of each beam vanishes after the cracking torque.

Figure (10) illustrates the behaviour of the reinforced concrete beam T1. The angle of twist at which the linear behaviour of the beam vanishes is 0.36^o. The the maximum twisting angle is 3.68^o. The slope of the torque-angle of twist relationship was calculated to determine the torsional stiffness of the beam. For the uncracked section, the value of the torsional stiffness is 19.23×10^3N.m/degree, which is the maximum value in this group of specimens at this stage of loading. The 8 mm stirrups reached their yield value at point e on Figure (10). The stirrup yielding was followed by the yielding of the 16 mm bars (point c in the Figure). The ultimate torsional capacity of the beam T2 was 21.25 kN.m which is 1.11 larger than the value of the beam T1.

Table 3 Test results for specimens

Beam designation	First crack load (kN.)	Maximum load (kN.)	First crack torque T_{cr} (kN.m)	Maximum torque T_u (KN.m)	T_{cr}/T %
T1	10.5	29.1	6.90	19.11	36
T2	12.6	32.4	8.25	21.25	39
T3	14.3	37.0	9.38	24.25	39

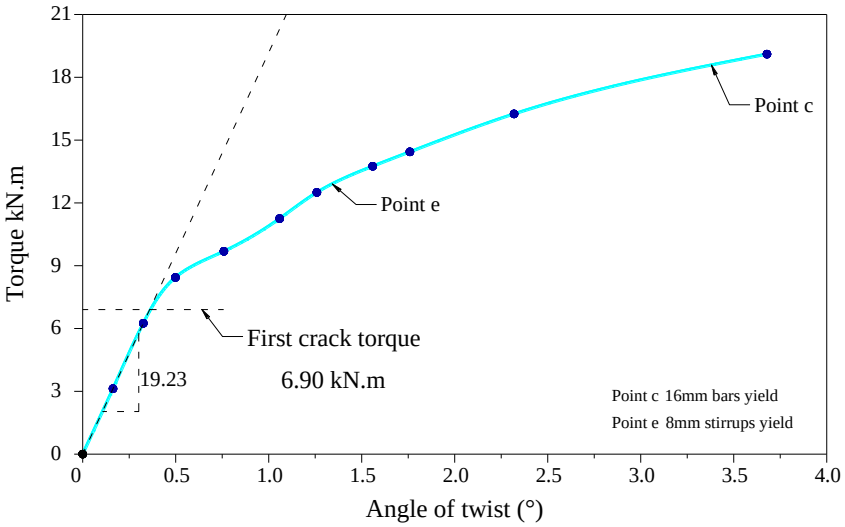

Figure (10) Torque -angle of twist relationship for reinforced concrete beam T1

Figure (11) shows the torque versus angle of twist relationship for CRC beam T2. From the figure the values of the angle of twist at which the linear behaviour of the beam vanishes and maximum twisting angle are 0.45^o, and 4.3^o respectively. The torsional stiffness of the beam for the uncracked section stage is 18.66×10^3 N.m/degree which is 97% of the value for the RC beam T1 at the same loading stage. The difference in post-cracking torsional stiffness value between the RC beam T1 and CRC beam T2 may be due to the contribution of the steel T-section. The strains from the strain gauge rosette readings showed that the steel T-section yielding occurs at a torque of 16.92 kN.m, point a on Figure (11). The 8 mm stirrups attained their yield strain at a torque equal to 17.64 kN.m, point a on Figure (11). The ultimate torsional capacity of this beam was 24.35 kN.m which is 1.27 larger than the value of the beam T1..

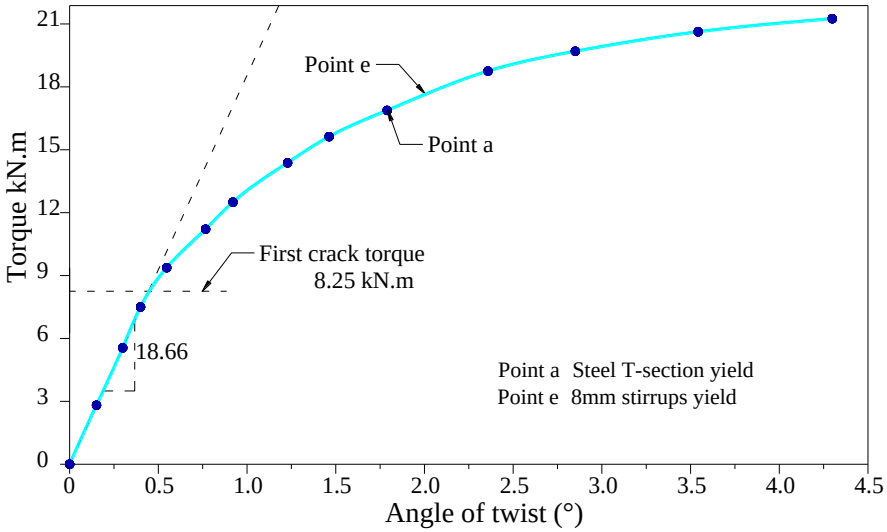

Figure (11) Torque -angle of twist relationship for CRC beam T2

Figure (12) shows the behaviour of the CRC beam T3, from which the values of the angle at which the linear behaviour of the beam vanishes and maximum twisting angle are 0.5^o and 3.68^o, respectively. The ultimate twisting angle of the beam was the same as that for the reinforced concrete beam and less than by 14.4% of that of the CRC beam T2 with a 100% degree of shear connection. The torsional stiffness of the beam before cracking torque was 18.95×10^3 N.m/degree which is 98.5% of the value for the RC beam T1 and 102% of the value for the CRC beam T2

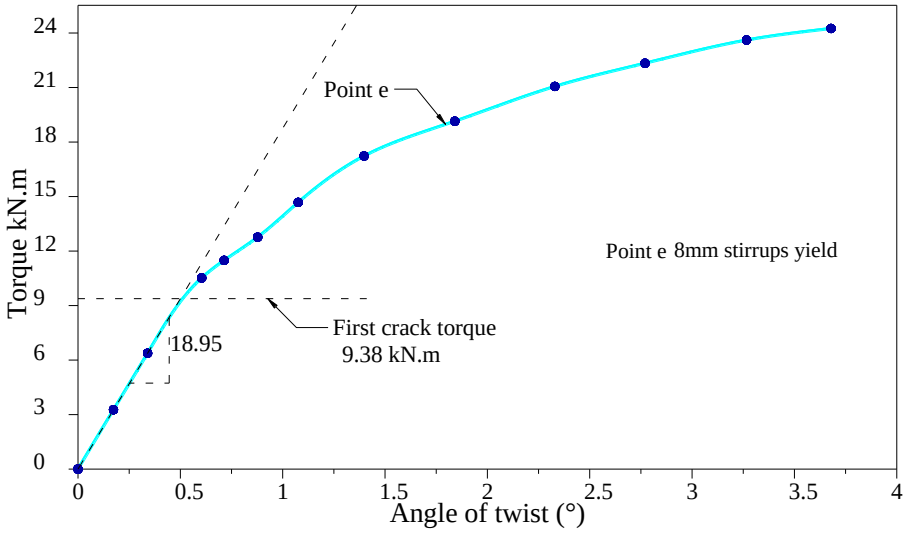

Figure (12) Torque - angle of twist relationship for CRC beam T3

Table 4 summarizes the results for the test beams. It can be seen from the results that for the uncracked section the torsional stiffness of the three beams are approximately the same. This may be attributed to the fact that before concrete cracking the contribution to the stiffness is confined to the concrete and the three beams have the same cross section dimensions and have the same concrete compressive strength.

Table 4 Angle of twist, and torsional stiffness values for the specimens

Beam designation	First crack angle of twist w_{cr}^o	Ultimate angle of twist w_u^o	Torsional stiffness Uncrack section $\times 10^3$N.m/degree
T1	0.36	3.68	19.23

T2	0.45	4.30	18.66
T3	0.51	3.68	18.95

Figures (10) to (12) show two distinct stages after the first linear relation. The first stage is characterized by a moderate deviation from the uncracked stage. However, in the second stage, which represents the stage before final collapse, the angle of twist becomes greater for small increments in applied torque. This behaviour is identical for the three beams, although it is more pronounced in CRC beams.

3 Finite element analysis

The RC and CRC beams were modelled using the finite element analysis program ABAQUS [Simulia, 2014]. Due to symmetry of load, boundary conditions and beam geometry, only half of the beam was modelled as shown in Figure (13).

A 20-node brick element C3D20R was used from the element library of ABAQUS to model the concrete, steel T-section, 8 mm stirrups, 8 mm longitudinal bars and 16 mm bars. A mesh convergency study has been conducted by changing the element size until no further influence on the results is obtained. The final size of elements selected for the model of concrete section was (9.4×10×10 mm) as shown in Figure (13). The element size for the steel T-section is shown in Figure (13-b). The length in longitudinal direction, z, is 50 mm. The discretization of the 8 mm and 16 mm bars is shown in Figure (13-c). The element lengths in z-direction are 20 mm and 40 mm for the two bar sizes 18 mm and 16 mm, respectively. The aspect ratio for all elements is kept to be about 10.

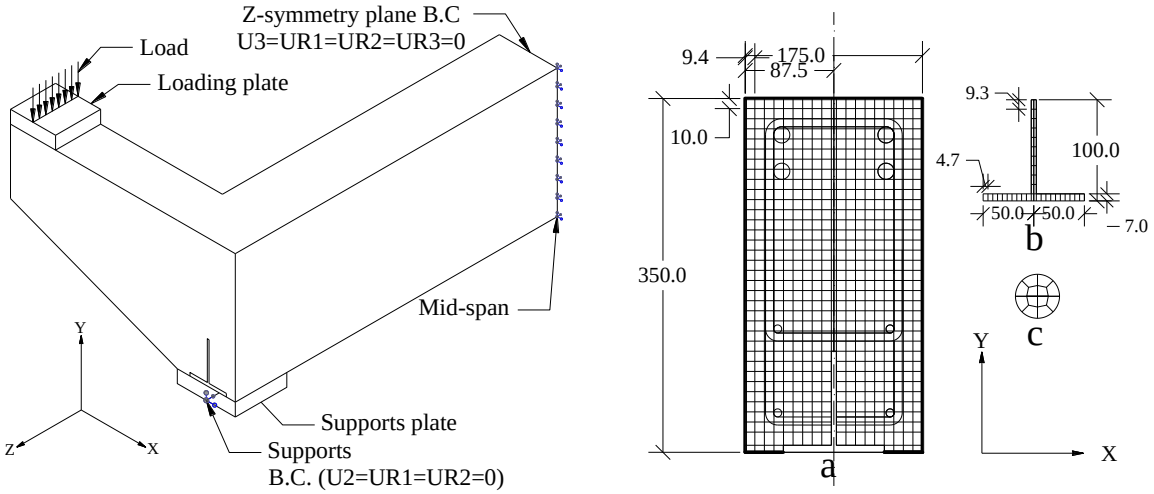

U: 1, 2, 3= Translation in x, y, and z directions, respectively
UR: 1, 2, 3= Rotation about x, y, and z directions, respectively

All dimensions are in millimeters

Figure (13) Beam boundary conditions and mesh size for beams

4 Material modelling

4.1 Concrete

Elastic-plastic behaviour that includes softening has been used according to Carreira and Chu [Carreia and Chu, 1985] to model concrete in compression. The parameters of the concrete model are listed in Table 5. The stress-strain relationship for concrete in tension is assumed linear up to the point of concrete cracking. The ratio of the second stress invariant on the tensile meridian , to that on the compressive meridian K were taken 0.667. The ratio of initial equiaxial compressive yield stress to initial uniaxial compressive yield stress were used as 1.16 which is the default value.

Table 5 Material parameters of Concrete damage plasticity model

Parameter	Value
Concrete compressive strength f′c	29.6 MPa
Concrete tensile strength	1.56 MPa
Modulus of elasticity E	25570 MPa
Poisson ratio ν	0.19
Dilation angle β	36^o
$f = f_{b0}/f_{c0}$	1.16
K	0.667

4.2 *Steel*

The Elastic-plastic model is used to model the behaviour of all types of the steel. The values of yield stress and ultimate strength of the steel T-section and reinforcement bars are as listed in Table 2.

4.3 *Interaction between beam components*

In the new composite reinforced concrete, the shear connection is provided throughout the length of the beam by relying on the stirrups which pass through drilled holes in the web of the steel T-section. The shear connection transmits the longitudinal shear force between the steel T-section and the concrete component of the beam. In the finite element model the shear connection was modelled by using a linear spring element of zero length with specified stiffness.

The positions of the spring elements coincided with the positions of the stirrups. Three springs in the three directions x, y, and z were used in each position. The stirrups were cut and connected to the web of the steel T-section by the spring elements on both sides of the web. The stiffness used in the model was based on the values mentioned in Refs. [Taylor, 1977], [Taylor et al., 1974], [Josef and Peter, 2000] [Shim et al., 2004], and [Prakash et al., 2012]. The chosen value for spring stiffness was 428 kN. /mm.

5 Validation of the finite element model

In order to validate the suggested finite element model, comparison with the experimental results of tested beams was made. Table (6) summarizes the comparison between the model and test results in terms of the torsional strength of beams. The ratios of results, experimental to model, are approximately one indicating good predictions of the strength.

Also, the finite element model and experimental results are compared in Figures (13) to (15) in terms of torque-angle of twist relationships. The figures depict excellent agreement in the response over the entire loading profile until failure.

Table 6 Experimental and F.E. model results for the beams

Beam designation	Experimental torque T_{ex}(kN.m)	F.E. model torque $T_{F.E.}$ (kN.m)	$T_{ex}/T_{F.E.}$ %
T1	19.11	18.95	101
T2	21.25	21.24	100
T3	24.25	23.75	102

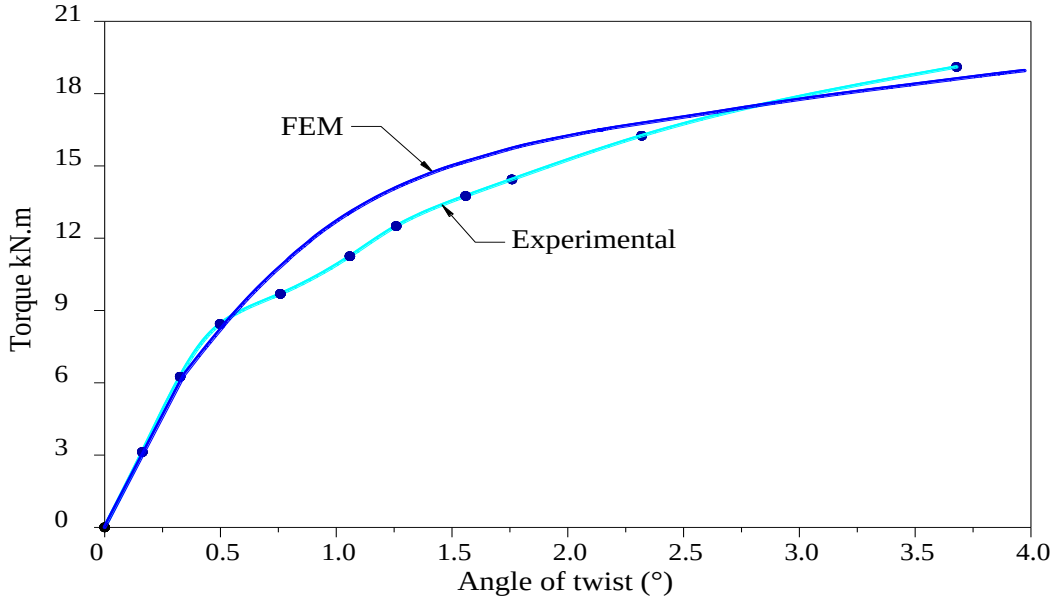

Figure (14) F.E model and experimental torque-angle of twist behaviour for reinforced concrete beam T1

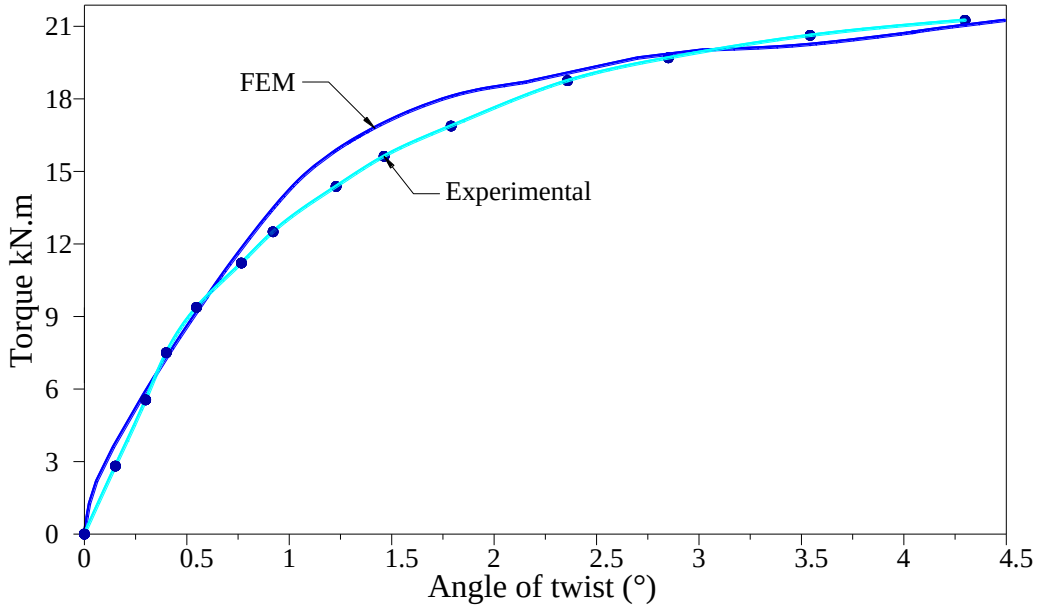

Figure (15) F.E model and experimental torque-angle of twist behaviour for beam T2

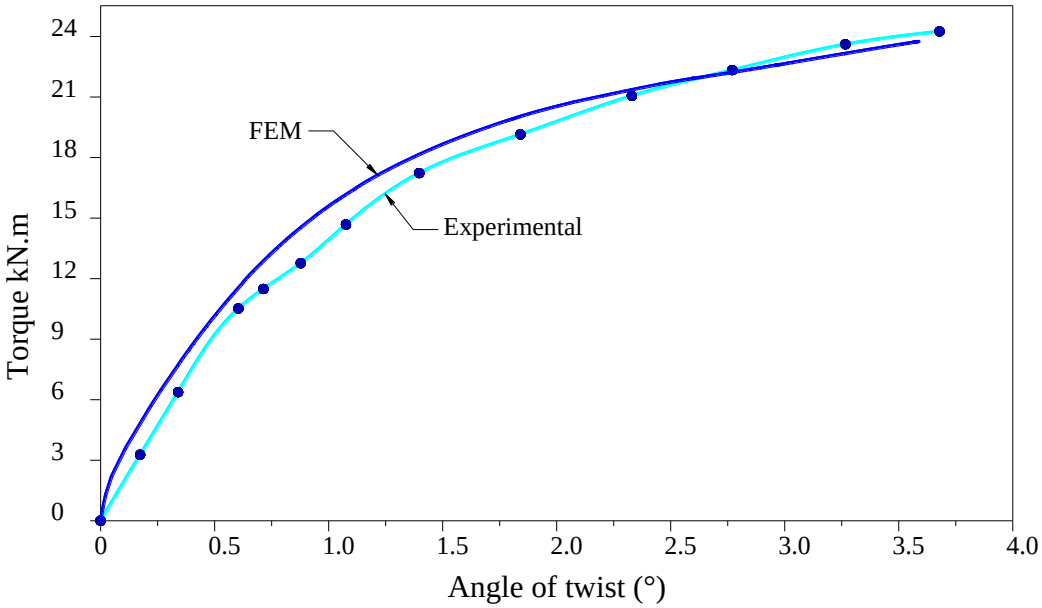

Figure (16) F.E model and experimental torque-angle of twist behaviour for beam T3

6 Parametric study

In any composite structural material, the increase of the connection between its components leads to an increase in strength and a reduction in deformations. The experimental test of CRC beams revealed larger torsional strength for beam T3 than beam T2. This was found although the degree of shear connection for beam T2 is the larger. For this reason, the verified finite element model was used to conduct a study to explore the effect of degree of shear connection on torsional strength of CRC beams. The selected degrees of shear connection were 14.3%, 18.4%, 26.5%, 34.7%, 65.3%, 73.5%, 81.6%, and 85.7%. The connection degree was changed by varying the number of stirrups used as shear connectors.

The results of the finite element analysis are shown in Table (7). It is clear from the results that under pure torsion loading the degree of shear connection has no effect on the strength of the CRC beams. A similar finding was obtained by Tan and Uy [Tan and Uy , 2011] for normal steel concrete composite beams.

Table 7 F.E model results for the CRC beams with different degrees of shear connection

Beam designation	Degree of Interaction %	Maximum torque from F.E. model kN.m
T2	100	21.2
T86	86	21.8
T82	82	22.0
T74	74	22.6
T65	65	23.0
T3	48.8	23.8
T35	35	24.0
T27	27	23.9
T18	18	23.9
T14	14	23.8

7 Comparison between the ACI 318-19 code, and experimental load capacity

The torsional capacity of the beams is calculated using ACI-19 equation 22.7.6.1a[ACI, 2019] re-written as Eq. (1) below:

$$T_n = \frac{2A_o A_t f_{yt}}{s}\cot\theta \qquad (1)$$

where

A_o: The gross area enclosed by the shear flow path, is taken as $0.85A_{oh}$ as recommended by ACI-14 code, article 22.7.6.1.1 [ACI, 2019]. A_{oh} (= $x_1 \times y_1$) is the area enclosed by the outermost legs of stirrups as shown in Figure (17).

A_t : area of one leg of the stirrup (50.2 mm^2).

f_{yt}: is the yield strength for the 8 mm stirrups (314 MPa).

s: is the stirrups spacing equals 60 mm,

θ: is taken equal to 45 as recommended by ACI-19 code 22.7.6.1.2 [ACI, 2019].

Therefore, the value of torsional strength for the CRC beams is calculated, by Eq. (1), as follows:

$$T_{n_{CRC}} = \frac{2 * (0.85 * 127 * 295) * 50.2 * 314}{60} * \cot 45 = 16.73\ kN.m \qquad (2)$$

and for RC beam

$$T_{n_{RC}} = \frac{2 * (0.85 * 127 * 302) * 50.2 * 314}{60} * \cot 45 = 17.13\ kN.m \qquad (3)$$

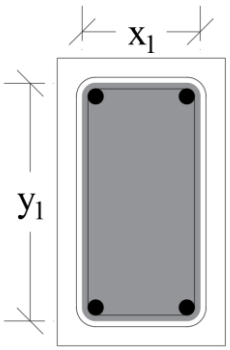

A_{oh}= shaded area

Figure (17) Area enclosed by the outermost legs of stirrups

By considering the steel T-section as regular reinforcement, the calculated torsional strength is 0.79 of the experimental value for beam T2 and 0.89 of the value for beam T3. This indicates that the ACI-19 code equation underestimates the torsional capacity of the beam because of ignoring the contribution of the steel T-section. For the RC beam T1 the ratio of torsional strength calculated using the ACI equation is 90% of the experimental value. The increase in torsional capacity of CRC beams above the values given by ACI-19 code is due to the strengthening provided by the flange of the steel T-section which acts as a strengthening steel plate to the reinforced concrete [Holman, 1982], [Shalaby, 2020]. In this study the ratios of experimental to ACI code results are 1.27 and 1.45 for beams T2 and T3, respectively. Such increases in torsional capacity of reinforced

concrete beams strengthened by steel plates were obtained in Refs. [Shalaby, 2020], [Khalil et al., 2017].

8 Conclusions

A new composite reinforced concrete CRC beams, in which a steel T-section acts as a reinforcement to concrete section, was proposed. The stirrups required to resist the applied shearing forces and torsion were used as connectors to transfer the horizontal shear between the concrete and the T-section. Experimental tests and finite element analysis were conducted to investigate the behaviour of beams, fabricated from this construction material, under pure torsion. The number of stirrups used as shear connectors was varied to explore the effect of degree of shear connection between the concrete and T-section on the strength behaviour. The program included testing one conventional reinforced concrete beam and two CRC beams with 100% and 48.8% degrees of shear connection. From the conducted study, it is found that:

1- The torsional strength of CRC beams is greater than that of RC beams. An increase of 27% is recorded for beam T3.
2- The degree of shear connection is found to have no effect on the torsional strength of the CRC beams under pure torsion.
3- The uncracked torsional stiffness for RC beam and CRC beams is approximately the same.
4- The ACI318-14 code underestimates the torsional strength of CRC beams. This may be attributed to the strengthening effect of the flange of the steel T-section at the soffit of beams.

9 References

ACI (American Concrete Institute) , 2019, Committee 318, “Building code requirements for structural concrete and commentary (ACI 318-19)”, Farmington Hills, MI, USA.

Carreia D. J. and chu K. H., 1985,”Stress-strain relationship for plain concrete in compression,” ACI Jornal, vol. 82, no. 6, pp.797-804.

Dolfocar U. W. and Nabeel. A. J., 2021, “Assessment of the flexural capacity of composite reinforced concrete beams using experimental tests and finite element analysis,” Journal of Physics: Conference Series, pp. 1–15.

Dolfocar U. W., 2021,“Experimental and theoretical study on composite reinforced concrete beams curved in plan.,” Ph. D Thesis, University of Basra, Iraq.

Ghosh B. and Mallick S. K., 1979, “Strength of steel–concrete composite beams under combined flexure and torsion.,” Indian Concrete Journal, vol. 53, no. 2, pp. 48–53.

Holman J. W., 1982, “Steel plates for torsion repair of concrete beams,” Journal of Structural Engineering, vol. 110, no. 1, pp. 10–18.

Josef H. and Peter D., 2000, “High performance steel and high performance concrete in composite structures,” Composite Construction in Steel and Concrete IV. pp. 891–902.

Khalil G. I., Debaiky A. S., Makhlouf M. H., and Ewis A. E., 2017, “Torsional behavior of reinforced concrete beams repaired or strengthened with transversal external post–tension elements.”, International Journal of Science Technology & Enqineering, vol. 4, Issue 4, pp. 54-73.

Prakash A., Madheswaran A. N, C., and Lakshmanan N., 2012, “Modified push-out tests for determining shear strength and stiffness of HSS stud connector-experimental study,” International Journal of Composite Materials, vol. 2, pp. 22–31.

Shalaby A. R., 2020, “Repair of RC beams with openings subjected to torsion using steel plates,”, M.Sc thesis, Cairo University.

Shim C. S., Lee P. G., and Yoon T. Y., 2004, "Static behavior of large stud shear connectors," Engineering Structures, vol. 26, no. 12, pp. 1853–1860.

Simulia D. S., 2014, "Abaqus 6.14," Abaqus 6.14 Analysis User's Guide.

Tan E. L. and Uy B., 2011, "Nonlinear analysis of composite beams subjected to combined flexure and torsion," Journal of Constructional Steel Research, vol. 67, pp. 790–799.

Taylor R. and Cunningham P., 1977, "Tests on the transverse bar shear connector for composite reinforced concrete," Proceedings of the Institution of Civil Engineers, part 2, vol. 63, pp. 913-920.

Taylor R., 1979, Composite Reinforced Concrete. Thomas Telford Limited, London, UK.

Taylor R., Clark D. S. E., and Nelson J. H., 1974, "Test on a new type of shear connectors for composite reinforced concrete," Proceedings of The Institution of Civil Engineers, Part 2, vol. 57, p. 177.

10 Appendix A: Notation

Symbol	Definition
f_{yt}	Yield strength of the stirrups
A_o	The gross area enclosed by the shear flow path
A_{oh}	The area enclosed by the stirrups
A_t	Area of one leg of the stirrup (50.2 mm^2)
s	Stirrup spacing
T_n	Torsional capacity of the R.C. section
$f'c$	Cylinder concrete compressive strength
f_{b0}	Initial equiaxial compressive yield stress
f_{c0}	Initial uniaxial compressive yield stress
K	Stress invariant ratio